LABORATÓRIO DE INSTRUMENTAÇÃO E FÍSICA EXPERIMENTAL DE PARTÍCULAS

LIP/02-03

ELECTRON BEAM ADJUSTMENT IN PLATO RTS 2 INCLUDING THE EFFECT OF AIR GAPS

M. C. Lopes[1], R. Paiva[1], A. Trindade[2], P. Rodrigues[2], L. Peralta[2,3]

[1] Centro Regional de Oncologia de Coimbra do IPOFG, 3000-075 Coimbra, Portugal

[2] Laboratório de Instrumentação e Física Experimental de Partículas, 1000-149 Lisboa, Portugal

[3] Faculdade de Ciências da Universidade de Lisboa, Portugal

Abstract

Background and Purpose: Beam characterization for electron dose calculations in PLATO RTS 2 treatment planning system requires the tuning of two adjustment parameters: $\sigma_{\theta x}$ (the initial angular spread) and FMCS (a "fudge" multiple Coulomb scattering parameter). This work provides a set of suggestions to optimise electron dose calculations with PLATO, taking into account the effect of air gaps between the electron applicator and the patient skin.

Material and Methods: Two adjustment criteria have been followed: one which uses just one input data set corresponding to the standard (null) air gap and another one that takes into account the whole range of clinically used distances between the electron applicator and the patient surface. The adjusted values of $\sigma_{\theta x}$ were compared with experimental data and GEANT3 Monte Carlo code results. A systematic study has been carried out of the effect of both adjustment parameters on electron dose calculations in water. Comparisons of dose distributions and point dose values have been done between PLATO RTS2, GEANT3 Monte Carlo code and experimental data. Also the dependence on field size has been assessed. The values of $\sigma_{\theta x}$ for the different electron energies obtained through the different approaches are discussed.

Results and conclusions: The first adjustment criteria yield unrealistic dose distributions whenever the air gap is different from the standard one. A $\sigma_{\theta x}$ balanced with a proper FMCS

parameter leads to reasonably good dose distributions and point dose values that agree with experimental results within less than 1%.

1. Introduction and Background

The process of commissioning and validation of treatment planning systems (TPS) has the aim of ensuring that the system is suitable for clinical use. This preliminary appreciation of a TPS should enable the assessment of its main features, possibilities, limitations and accuracy. It is an important step towards the overall quality assurance in radiotherapy [10, 14, 24]. The test data set should be as exhaustive as possible in order to fully cover the main clinical cases and thus correspond to as much a deeper inspection as the system allows.

Several task groups have produced recommendations and protocols for testing TPS [1, 3, 7] and many other papers have been published concerning several aspects of the quality assurance of TPS [4, 5, 18, 19], including criteria for acceptability of dose calculations [20]. Most of these studies are however restricted to photon dose calculations and concerning electron beams only a limited number of reports discuss them [3, 6, 12, 23].

The purpose of this work is to fully explore the beam adjustment process for PLATO (Nucletron) RTS version 2.5.2., concerning now electron beams. This widely used TPS is a Unix based system with software tools that enable the physicist to make convenient beam adjustments in order to improve the matching of calculated results with measured data.

The results of a quite deep inspection on the main features of the system (RTS version 2.1.) concerning photon beams have already been presented [16]. The test data set for that study involved open, wedged, blocked and asymmetric fields for four photon energies (4, 6, 18 MV and ^{60}Co) and using all the adjustment parameters available for beam modelling: fluence profile; gaussian width; beam hardening; wedge and block geometrical shapes; wedge, collimator and block attenuation coefficients; source-tray distance and tray transmission.

A first approach to electron beam adjustment (RTS version 2.3.3) has been made starting from the basic beam data set for the standard null air gap (meaning no additional distance between the electron applicator end and the patient or phantom surface) [17]. For electron beams just two adjustment parameters are available – the initial angular spread, $\sigma_{\theta x}$ and another parameter named FMCS (fudge multiple Coulomb scattering) that corresponds to a “fudge” parameter in the Hogstrom algorithm used in electron dose calculations [9].

The purpose of this work is to present the procedure followed in electron beam adjustment for PLATO RTS version 2.5.2. following a criteria that involved the simultaneous consideration of relative dose distributions (percent depth dose (PDD) and profiles at different depths) and also point dose values (output factors) for six electron energies and different field sizes, for air gaps up to 5 cm in 1 cm steps.

The influence of inputting basic beam data for different air gaps has been assessed through the dependence on PDD and output factor values.

Simultaneously and in order to appreciate the goodness of the experimental $\sigma_{\theta x}$ values obtained following the experimental procedure recommended in the user's manual, a MC simulation has been performed using GEANT3 code [8]. From the phase space distribution in the plan just below the electron applicator simulated values of $\sigma_{\theta x}$ have been obtained. Also isodose distributions reconstructed upon simulated dose matrices have been compared with experimental results for different air gaps.

In summary this work provides the practicing medical physicist who uses the commercial planning system PLATO with a set of suggestions to optimise electron dose calculations with this TPS. Furthermore the intrinsic limitations of the TPS are stressed, specially those with clinically relevant implications.

2. Methods and Materials

Routine dose calculations are performed at CROC-IPOFG, Coimbra (Portugal) using PLATO (Nucletron) TPS. Electron dose calculations in PLATO use the pencil beam (PB) model following the Hogstrom approximation using the Fermi-Eyges theory of multiple Coulomb scattering [9]. The algorithm needs to be fed with electron beam dosimetric data including for each field size and energy: percent depth dose curves (PDD), output factors (OF) and depths of measurement. For each energy, two other parameters are required as input data and those are the only two adjustment parameters for beam modelling: $\sigma_{\theta x}$ and FMCS. The latter arises in the Hogstrom construction as a "fudge" multiple Coulomb scattering factor to obtain a better agreement between calculated and measured data. Its default value is 1.0.

The parameter $\sigma_{\theta x}^2$ is the mean angular variance of the angular distribution projected onto the x-z plane at the level of the electron applicator end. The PB approach requires this quantity because the width of each PB at depth (σ^2) results from the addition of the initial angular spread at the bottom of electron applicator ($\sigma^2_{\theta x}$) and a component due to scattering in the medium (σ^2_{MCS}):

$$\sigma^2 (Z) = \sigma^2_{MCS} + (Z+L)^2 \sigma^2_{\theta x} \qquad (1)$$

The FMCS parameter, in the context of PLATO system (RTS2) is a multiplicative factor to the first term σ^2_{MCS}.

During the commissioning process $\sigma_{\theta x}$ values have been determined according to a Nucletron proposed methodology adapted from Hogstrom method, for the six electron energies produced by the Mevatron (Siemens) KD2 linear accelerator: 6, 8, 10, 12, 15 and 18 MeV. According to this methodology $\sigma_{\theta x}$ values were obtained through:

$$\chi = L\sqrt{2\pi}\,\sigma_{\theta x} \qquad (2)$$

where χ represents the penumbra width (90%-10%) of the off axis ratio profiles of a 15x15 cm^2 field size measured at a shallow depth (5mm) with a Markus chamber (PTW 23343) in a motorized water phantom (PTW MP3) and L the air gap between the end of the electron applicator and phantom surface. The $\sigma_{\theta x}$ values expressed in radians correspond to 0.391 times the slope of the line fitting the data, for each energy [9], as shown in Fig. 1.

(Fig. 1)

Eq. (2) derives from the assumption of a Gaussian angular distribution for the scattering process, where the scattering of electrons in the air layer between the bottom of the electron applicator and the phantom surface is neglected. The penumbra width of the beam profiles is thus related to the spatial variance of fluence distribution [2].

Using validated phase space files [21,22] obtained with GEANT3 (version 3.21) code, simulated angular distributions for the 10x10 cm^2 field size were obtained and fitted with a Fermi-Eyges distribution for the plane immediately below the electron applicator (Fig.2).

(Fig. 2)

Derived $\sigma_{\theta x}$ values from Monte Carlo agrees with experimental method with differences less than 8.0 mrad (Table 1).

(Table 1)

The process of $\sigma_{\theta x}$ adjustment in Plato followed two different approaches. The first procedure (named here procedure A), suggested by Nucletron and commonly followed by centres where just one input beam data set is available (usually corresponding to the standard air gap) is to tune $\sigma_{\theta x}$ in order to fit the width of higher level isodose curves (> 80%) to experimental data for each energy. This is the unique criteria for the $\sigma_{\theta x}$ adjustment. FMCS is kept equal to unity. The adjusted $\sigma_{\theta x}$ values obtained are ten fold higher than those determined from the experimental procedure for all six energies.

The second approach (procedure B) followed a different criteria. Starting from the $\sigma_{\theta x}$ values experimentally determined, and giving as input experimental PDDs and OFs for air gaps up to 5 cm, both $\sigma_{\theta x}$ and FMCS have been tuned. The adjustment criteria corresponded to a compromise between dose distributions assessed by dose profiles at different depths for each air gap and keeping a good dose description at the beam central axis (PDD). Also point dose values (OF) are inspected in order not to deviate more than 2 % from experimental results. This detailed study has been carried out for 10 MeV and a 10x10 cm^2 field size. The final values for $\sigma_{\theta x}$ are much closer to experimental ones (see Table 1). However they are still higher than these and also higher than those obtained from MC simulation. The discussion on these results is done below.

3. Results and discussion

3.1. Relative dose distributions

Using the experimental values of $\sigma_{\theta x}$ for beam modelling in PLATO, we have concluded that they are clearly too small to adequately describe dose distributions in water, underestimating the electron spread. Higher level isodoses (above 80%) are much larger than experimental ones and the opposed tendency is shown by lower level isodoses (below 30%). If FMCS is increased to its maximum allowed value (FMCS=2) the elastic scattering in water is enhanced but not enough. The higher level isodoses became narrower but still larger than the experimental ones and no effect was observed concerning the wrong behaviour with increasing air gaps.

Following the tuning criteria for $\sigma_{\theta x}$, denominated procedure A, it led to $\sigma_{\theta x}$=0.4 rad for E=10 MeV whereas the measured $\sigma_{\theta x}$ is just 0.046 rad. FMCS was kept equal to unity as suggested by Nucletron. We can see in Fig. 3a that the calculated dose distribution follows closely the experimental values for air gap zero, specially for depths close to dmax (the depth of adjustment). For shallow depths the isodoses tend to be narrower and for larger depths the lower level isodoses (<30%) are larger. This is an expected tendency of dose calculations because the algorithm does not take electron absorption into account. Increasing the air gap between the electron applicator and the phantom surface with this beam modelling completely unrealistic isodose distributions are obtained as we can see in Fig. 3b, for air gap of 4 cm. Not even at the beam central axis is the dose correctly calculated (Fig. 3c).

(Fig. 3)

Having this dependence of dose distribution with air gap as a main worry for $\sigma_{\theta x}$ and FMCS tuning, through procedure B the system is fed with different input data sets for each air gap. Then a systematic increasing of $\sigma_{\theta x}$ has been done starting with the experimental values and evaluating for each $\sigma_{\theta x}$ trial the effect of increasing FMCS within its limits. This detailed study has been done for E=10 MeV. The best agreement was achieved for $\sigma_{\theta x}$ = 0.1 rad and FMCS=2.

With this choice of parameters isodose lines calculated with PLATO can reasonably follow the experimental data with increasing air gap. The results for air gaps of 1 and 4 cm are presented in Fig. 4a and 4b. Still no good dose distribution is achieved at shallow depths.

(Fig. 4)

It is clear that this value of the adjustment parameter $\sigma_{\theta x}$ is still too small to follow the experimental dose values in water but its influence on dose calculation for increasing air gaps leads to reasonably good results. The lack of electron absorption or energy-loss model to account for inelastic scattering interactions in the Hogstrom algorithm, as an opposed influence, is more clearly visible at larger depths. If we compare Fig. 3b and 4b we can clearly see that a too large value of $\sigma_{\theta x}$ (procedure A) results in an abnormal spread in dose distribution whenever there is an air gap between the electron applicator and the phantom surface which is reinforced by the lack of electron absorption. The second tuning (procedure B) prevents this spreading to occur by keeping a low value for $\sigma_{\theta x}$ and compensating it by the increase of elastic scattering in the medium through the value of FMCS. This is a good compromise between these opposed influences.

In Fig. 5a and 5b we can see that isodoses reconstructed from dose distributions simulated with GEANT3 reproduces the experimental data very accurately either with or without air gap.

(Fig. 5)

The larger influence of applicator scatter on the dose profiles obtained for small air gaps is used in [2] to derive an "effective" $\sigma_{\theta x}$ which according to Battum and Huizenga follows a relationship where $\sigma_{\theta x}^2/T(E_0)$ is constant for each type of accelerator. $T(E_0)$ is the linear angular scattering power in air and E_0 the mean energy at the phantom surface as given by ICRU Report 35 [10]. The values of $T(E)/\rho$ has been recalculated by Li and Rogers [15] using the Molière multiple scattering distribution and taking the Moller scattering effect into account. These authors report values of up to 22% higher than those reported by ICRU 35 for low-Z materials and energies less than 60 MeV. It is however remarkable that the dependence on E of $T(E)/\rho$ reported:

$$T(E) \propto E^{-n} \qquad (3)$$

where n=1.77 for air in the energy range of 5-20 MeV, leads to a dependence of:

$$\sigma_{\theta x} \propto E^{-0.886} \qquad (4)$$

when we use the constant relation claimed in [2]. If we apply this power law to the $\sigma_{\theta x}$ values obtained in procedure B we find exactly the same n=0.886. The reason for the disagreement between the experimental values of $\sigma_{\theta x}$ and the adjusted ones could thus derive from a scale factor.

3.2. Point dose calculations

Concerning point dose values and aiming to obtain OFs with deviations below 2% [23] when compared with experimental results for air gaps within the clinical used range we have concluded that procedure A does not achieve this objective for air gaps greater than 1 cm. Also it is not enough to introduce the correct OF value as an input parameter (procedure A with input data sets for each air gap), for there are still differences up to 7%, depending on electron energy (see Table 2 for E= 8 MeV). This clearly results from the influence of $\sigma_{\theta x}$ value on dose descriptions at the beam central axis. With the parameter settings resulting from procedure B we finally got OFs that agree with measured ones within less than 1% for all energies.

(Table 2)

It should be stressed that the influence of $\sigma_{\theta x}$ value on PDD curves is much stronger for lower energies. This is because the buildup region is much more pronounced for these energies. For higher energies (above 12 MeV) the extended dose plateau enables the point dose to be quite insensitive to the depth of maximum dose, where the OF is defined. What we have experimentally verified is that PDDs do not change with air gaps up to 5 cm. Procedure A, leading to distorted dose distributions namely at the beam central axis (see Fig. 6a) yields, for the lower energies, to variable build up regions which determine OFs much different from experimental ones.

(Fig. 6)

In order to meet the user's interest, we have tested the beam modelling dependence on $\sigma_{\theta x}$ value independently of inputting extra beam data sets for different air gaps. We have concluded that even without extra input data, if the parameters $\sigma_{\theta x}$ and FMCS are properly adjusted, both PDDs and OFs keep within reference acceptability criteria [23].

In Fig. 7a we compare, for E= 10 MeV, OF results from measurements, procedure A, procedure B (with and without input data sets for different air gaps) and MC simulation. Also in the same figure we have plotted the 2% per centimetre decreasing dependence on air gap referred by Klevenhagen [13]. It shows a good agreement both with measurements and with procedure B. MC values are within 1.2% deviations from measurements.

(Fig. 7)

3.3. Field size dependence

To complete the study we have tested the $\sigma_{\theta x}$ and FMCS final values for different field sizes (5x5 and 20x20 cm^2). Despite the fact that a field size dependence of $\sigma_{\theta x}$ has been reported by some authors [2], the present implementation of PLATO algorithm for electron dose calculations considers $\sigma_{\theta x}$ just a function of electron energy. The followed procedure for beam adjustment proved to lead to PDDs and OFs values within the accepted tolerance for electron dose calculations at the beam central axis for the available electron applicators and for air gaps within the clinical used range. The linear decreasing of OFs with air gaps up to 5 cm has also been obtained for different field sizes (see Fig. 7b). All the other conclusions about field size dependence for electron beams that have previously been assessed [17] remained unchanged and also valid for increasing air gaps.

4. Conclusions

Electron beam modelling in PLATO RTS 2 (version 2.5.2.) has been deeply explored taking into account how the air gap between the electron applicator and the patient surface affects dose calculation. The beam adjustment parameters for this widely used TPS - $\sigma_{\theta x}$ and FMCS – have been tuned and their effect on dose calculation in water has been assessed. The initial angular variance $\sigma_{\theta x}^2$ is a measure of the electron angular spread at the bottom of the electron applicator and its value is of major influence for dose calculation in water. FMCS is a second order adjustment parameter that affects the electron elastic scattering in the irradiated medium and derives from the Hogstrom algorithm implemented in PLATO.

The $\sigma_{\theta x}$ values obtained following different adjustment criteria have been discussed. Also $\sigma_{\theta x}$ values obtained through the phase-space distribution simulated with GEANT3 Monte Carlo code have been assessed. The results of MC simulation for dose calculations in water follow experimental data very accurately for the whole range of air gaps.

The present study ends up on a set of suggestions to achieve optimised electron dose calculations with PLATO RTS 2:

a) The adjustment criteria for $\sigma_{\theta x}$ based exclusively on the width of higher level isodoses at the depth of maximum dose are insufficient to correctly model dose distributions whenever there is an air gap different from the standard one, to which the input data set corresponds. Too large values of $\sigma_{\theta x}$ are obtained using this adjustment procedure (ten-fold higher), leading to an exaggerated dose spread with increasing air gaps. Also wrong values of output factors are obtained with deviations largely exceeding 10%, depending on beam energy.

b) The experimental procedure recommended in PLATO user's manual leads to $\sigma_{\theta x}$ values that are too small to achieve a proper beam modelling. It is a better choice to use the procedure as a starting point for just one of the electron energies available (preferably an intermediate one) and then tune the adjustment of $\sigma_{\theta x}$ in order to achieve good line dose descriptions and output factors for the whole range of clinical used air gaps. After this intermediate $\sigma_{\theta x}$ value has been found a power law dependence given by $\propto E_0^{-0.886}$, where E_0 is the mean energy at the phantom surface, can be used for the whole range of energies.

c) The value of $\sigma_{\theta x}$ should be balanced by a proper value of the FMCS parameter, meeting the same criteria. This parameter, increasing the weight of electron elastic scattering in water will balance, together with the lack of electron absorption valid for the present electron dose implementation in PLATO, the low value of the initial angular spread necessary to contain the dose spread for increasing air gaps.

d) Following this procedure for parameter tuning, the dose distribution at the beam central axis (PDD) and the OF values are quite insensitive to whether or not the system is fed with additional input data sets for different air gaps (at least up to 5 cm air gaps). Thus, PDDs keep unchanged with increasing air gaps and OFs deviate no more than 1 % from experimental values. Nevertheless, if the user wants to feed the system with data sets for different air gaps and if there are no experimental data available, then he (she) can input the same PDD for all air gaps as the PDD does not change with air gap. Also empirical OFs can be input using the 2% per centimetre decreasing linear law suggested by Klevenhagen [13] without causing calculated OFs to deviate more than 2% from experimental results.

e) The tuned values of $\sigma_{\theta x}$ and FMCS proved to work for all field sizes within the acceptability criteria for electron dose calculations.

The procedure followed for adjustment of $\sigma_{\theta x}$ and FMCS results from a suitable balance between different phenomena that affect in different ways electron dose calculations in water with PLATO TPS – the initial angular variance of the electron distribution and the electron absorption and scattering in water. The final values proved to give proper PDDs and OFs within 1% when compared with experimental results, for different energies, air gaps and field sizes. However the overall dose distribution, namely at shallow depths and at the beam edges, is not so satisfactory.

The compromise values lead to too narrow isodose distributions at the phantom entrance. This calculation result should be taken into account whenever the dose description close to the surface and near the beam edges has some clinical relevance. This is certainly the case when adjacent electron beams are to be used to cover for instance a large skin area (as in the case of scars). The decision on beam junction cannot be taken upon the dose calculation in PLATO. Using the possibilities PLATO is offering for fitting the electron beam data, it is not possible to obtain a compromise that offers sufficiently accurate modelling of the isodose distributions both at shallow depths and at the beam edges at larger depths.

REFERENCES

[1] American Association of Physicists in Medicine. Radiation treatment planning dosimetry verification. AAPM Report 55 of Task Group 23 of the Radiation Therapy Committee. Woodbury, NY: American Institut of Physics, 1995

[2] Battum L.J., Huizenga H. On the initial angular variances of clinical electron beams. Phys. Med. Biol. 1999; 44: 2803-2820.

[3] Brahme A., Chavaudra J., Landberg T., et al. Accuracy requirements and quality assurance of external beam therapy with photons and electrons. Acta Oncol. (Stockolm). 1988; Suppl. 1: 1-76.

[4] Caneva S., Rosenwald J.C., Zefkili S. A method to check the accuracy of dose computation using quality index: application to scatter contribution in high energy photon beams. Med. Phys. 2000; 27: 1018-1024.

[5] Craig T., Brochu D., Van Dyk J. A quality assurance phantom for three-dimensional radiation treatment planning. Int. J. Radiat. Oncol. Biol. Phys. 1999; 44: 955-966.

[6] Cygler J., Ross, J. Electron dose distribution in an anthropomorphic phantom – verification of Theraplan treatment planning algorithm. Med. Dos. 1988; 13: 155-158.

[7] Fraass B., Doppke K., Hunt M., et al. American Association of Physicists in Medicine. Radiation Therapy Committee Task Group 23 Quality assurance for clinical radiotherapy treatment planning. Med. Phys. 1998; 25: 1773-1829.

[8] Gianni S., Ravndal S., Maire M., 1994 GEANT – Detector Description and Simulation Tool, CERN – European Organization for Nuclear Research, CERN Program Library Long Writeup, W59013

[9] Hogstrom K.R., Mills M.D., Almond P.R. Electron beam dose calculations. Phys. Med. Biol. 1981; 26: 445-459.

[10] International Commission on radiation Units and Measurements (ICRU). Radiation dosimetry: electron beams with energies between 1 and 50 MeV. ICRU Report 35; 1984.

[11] International Commission on radiation Units and Measurements (ICRU). Use of computers in external beam radiotherapy procedures with high energy photons and electrons. ICRU Report 42; 1987.

[12] Khan F. M., Doppke K. P., Hogstrom K. R., et. al. Clinical electron-beam dosimetry: Report of AAPM Radiation Therapy Committee Task Group No 25. Med. Phys. 1991; 18: 73:109

[13] Klevenhagen S.C. In: Physics of electron beam therapy. Adam Hilger Ltd. Bristol and Boston. 1985; 85-88.

[14] Kutcher G.J., Coia L., Gillin M., et al. Comprehensive QA for radiation oncology: Report of AAPM Radiation Therapy Committee Task Group 40. Med. Phys. 1994; 21: 581-618.

[15] Li X.A., Rogers D.W.O. Electron Mass Scattering Powers: Monte Carlo and Analytical Calculations. Med. Phys. 1995; 22: 531-541.

[16] Lopes M.C., Couceiro M., Alves C., Chaves A. Commisioning and validation of treatment planning systems as part of quality assurance in radiotherapy. Rad. & Oncol. 1999; 52 (Supp. 1); S64.

[17] Lopes M.C., Preto F., Alves C. Electron Output factors for irregular fields following commissioning procedures in PLATO RTS 2. Proceedings of the Topical Meeting on Medical Radiation Physics and Engineering. Physica Medica. 2001; 17(Supp. 4): 20-22.

[18] Niermierko A., Goitein M. The influence of the size of grid used for dose calculation on the accuracy of dose estimation. Med. Phys. 1989; 16: 239-247.

[19] Panitsa E., Rosenwald J.C., Kappas C. Intercomparison of treatment planning systems (TPS) used in radiotherapy: progress report of the TPS group of the European Dynarad project. Proceedings Vth international conference of medical physics. Physica Medica. 1997; 13(Supp. 1): 139-143.

[20] Trindade A., Alves C., Chaves A., et al. Influence of air gaps on electron dose calculation, Proceedings of the 6th Biennial ESTRO Meeting on Physics for Clinical Radiotherapy. Rad. & Onc. 2001; 61 (Suppl. 1) S39.

[21] Trindade A., Rodrigues P., Alves C., et al. Monte Carlo Simulation of Electron Beams for Radiotherapy – EGS4, MCNP4b and GEANT3 intercomparision. Proceedings of the Monte Carlo 2000 Conference, Lisbon,, 23-26 October 2000, Kling, Barão, Nakagawa, Távora, Vaz (Eds.). 2001; 311-316.

[22] Trindade A., "Optimização do cálculo de dose por simulaçao Monte Carlo em radioterapia externa com feixes de electrões", MSc. Degree Thesis, Faculty of Sciences, University of Lisbon, 2002; http://www.lip.pt

[23] Van Dyk J., Barnett R.B., Cygler J.E., Shragge P.C. Commissioning and quality assurance of treatment planning computers. Int. J. Radiat. Oncol. Biol. Phys. 1993; 26: 261-273.

[24] World Health Organization (WHO). Quality Assurance in Radiotherapy. Geneva: WHO: 1988; 34-35.

Figure Captions

Fig. 1 – a) Penumbra width (90%-10%) of dose profiles as a function of air gap; b) $\sigma_{\theta x}$ values as a function of the nominal energy derived from the experimental procedure

Fig. 2 – Polar angular distribution corresponding to the phase space file at the bottom of the electron applicator for E= 10 MeV. $\sigma_{\theta x}$ is derived from the curve fitted with a Fermi-Eyges distribution.

Fig. 3 – Isodose distributions superimposed onto experimental data points for a 10x10 cm^2 field size and E=10 MeV calculated in PLATO (procedure A) for a) air gap 1 cm; b) air gap 4 cm. In c) the calculated percent depth dose curve (PDD) is shown for 4 cm air gap.

Fig. 4 – Isodose distributions superimposed onto experimental data points for a 10x10 cm^2 field size and E=10 MeV calculated in PLATO (procedure B) for a) air gap 1 cm; b) air gap 4 cm.

Fig. 5 – Isodose distributions reconstructed from MC simulation superimposed onto experimental data points for a 10x10 cm^2 field size and E=10 MeV for a) no air gap; b) air gap 4 cm.

Fig. 6 – Percent depth dose curves for different air gaps resulting from: a) procedure A; b) Procedure B

Fig. 7 – Output factors for E=10 MeV as a function of air gap. a) 10x10 cm^2 ; b) 20x20 cm^2

Table Captions

Table 1 - $\sigma_{\theta x}$ values derived from experimental procedure; from tuning procedures A and B and from MC simulation.

Table 2 – Output factors for different air gaps and resulting from different beam adjustments.

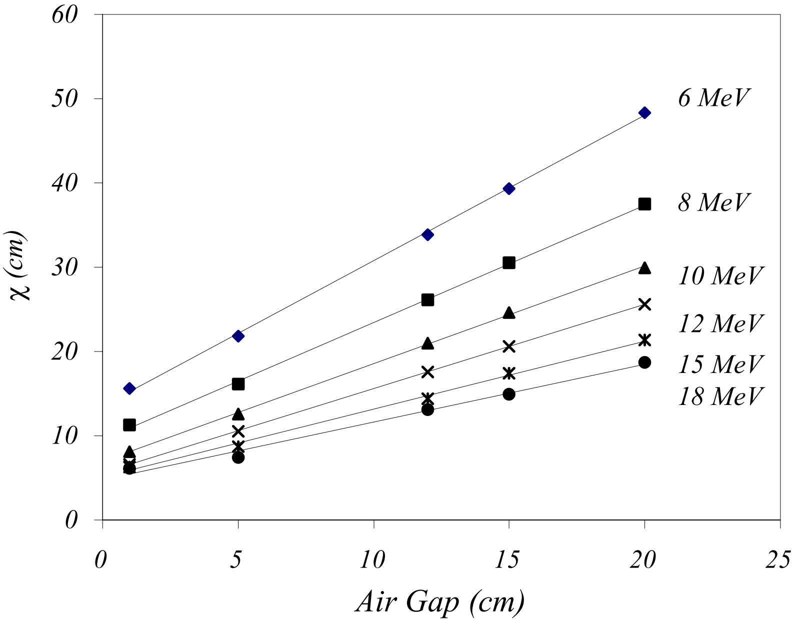
60
50
40
30
20
10
0
0
5
10
15
20
25
χ (cm)
Air Gap (cm)
6 MeV
8 MeV
10 MeV
12 MeV
15 MeV
18 MeV

Fig.1a)

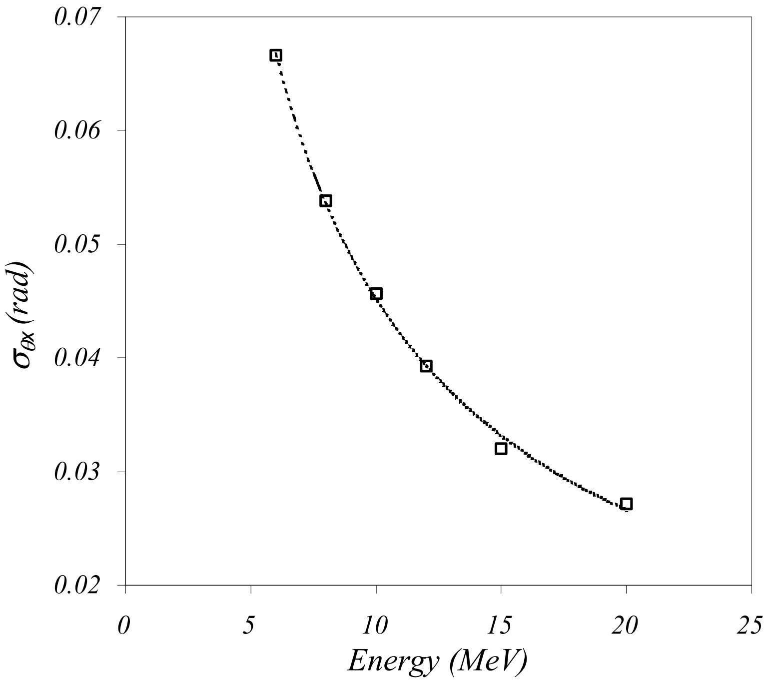
0.07
0.06
0.05
0.04
0.03
0.02
0
5
10
15
20
25
σθx (rad)
Energy (MeV)

Fig.1b)

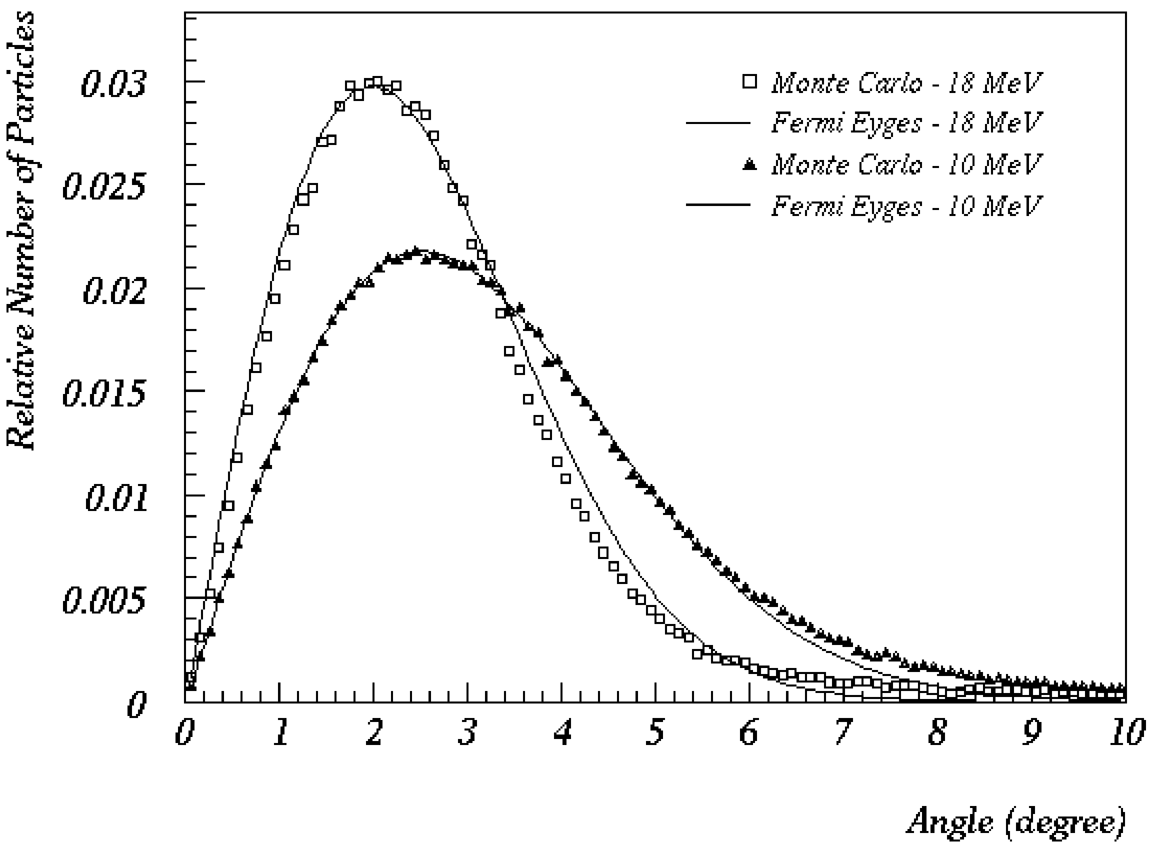
Relative Number of Particles
0.03
0.025
0.02
0.015
0.01
0.005
0
0
1
2
3
4
5
6
7
8
9
10
Angle (degree)
Monte Carlo - 18 MeV
Fermi Eyges - 18 MeV
Monte Carlo - 10 MeV
Fermi Eyges - 10 MeV

Fig. 2

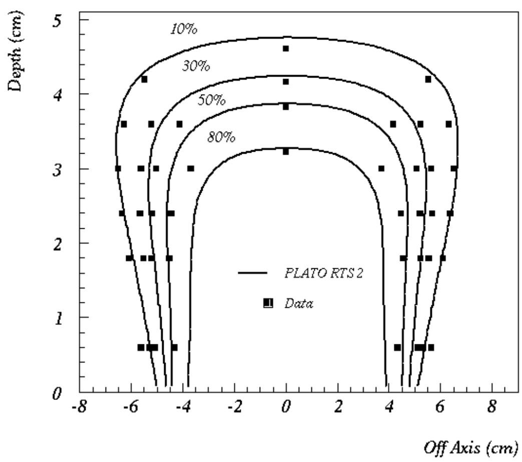

Fig. 3 a)

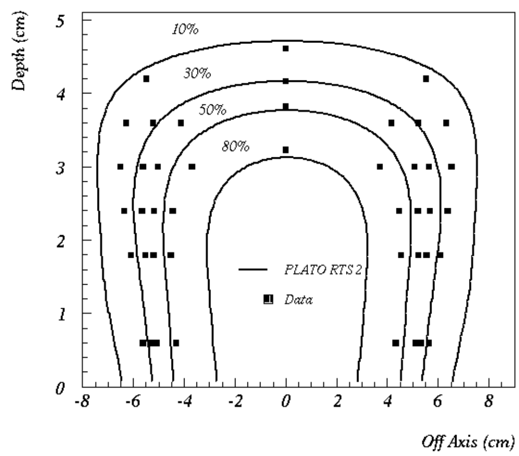

Fig. 3 b)

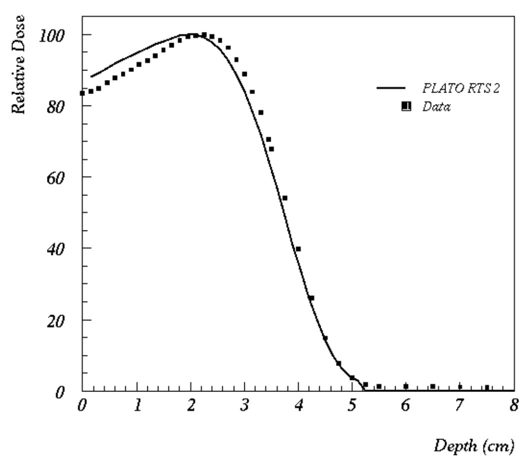

Fig. 3 c)

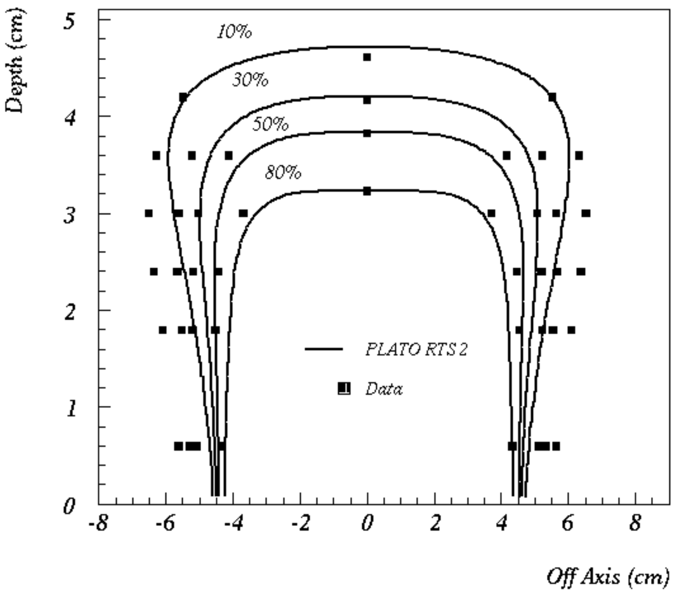
10%
30%
50%
80%
Depth (cm)
5
4
3
2
1
0
-8
-6
-4
-2
0
2
4
6
8
Off Axis (cm)
PLATO RTS 2
Data

Fig. 4 a)

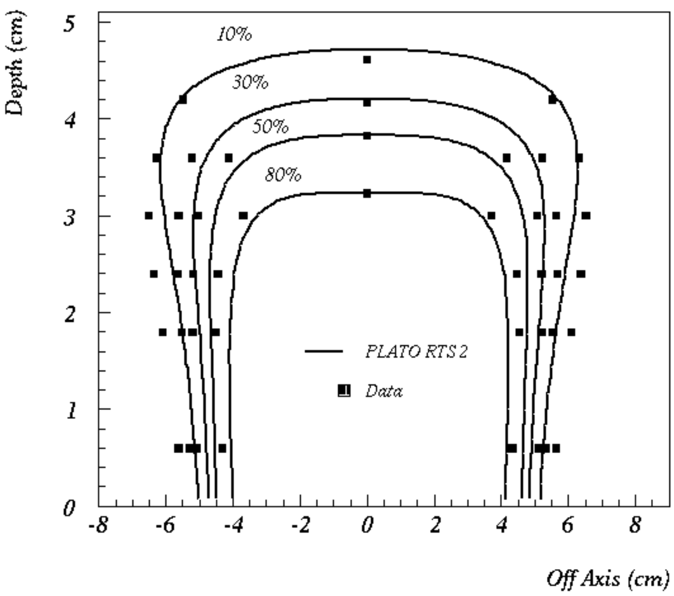
10%
30%
50%
80%
Depth (cm)
5
4
3
2
1
0
-8
-6
-4
-2
0
2
4
6
8
Off Axis (cm)
PLATO RTS 2
Data

Fig. 4 b)

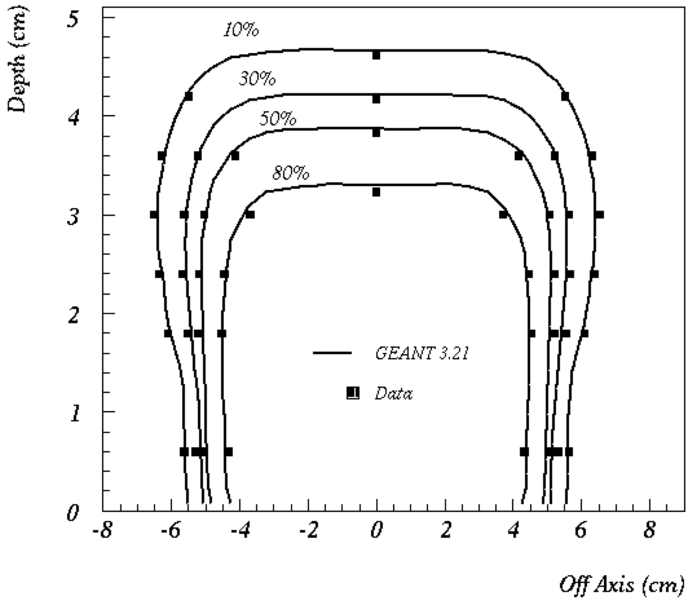
Depth (cm)
10%
30%
50%
80%
GEANT 3.21
Data
Off Axis (cm)

Fig. 5 a)

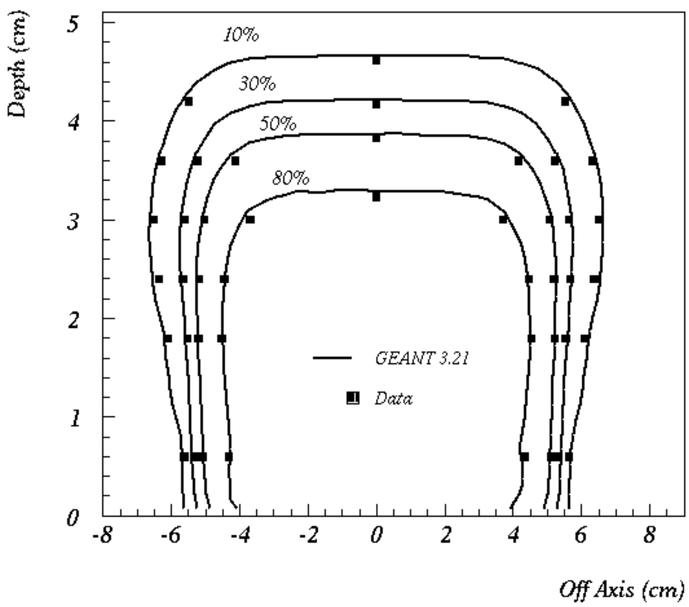
Depth (cm)
10%
30%
50%
80%
GEANT 3.21
Data
Off Axis (cm)

Fig. 5 b)

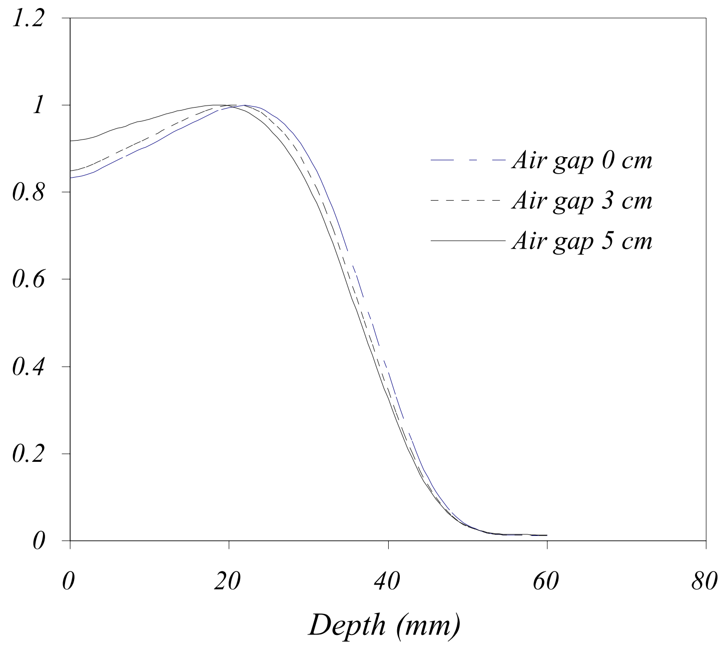

1.2
1
0.8
0.6
0.4
0.2
0
0
20
40
60
80
Depth (mm)
Air gap 0 cm
Air gap 3 cm
Air gap 5 cm

Fig. 6 a)

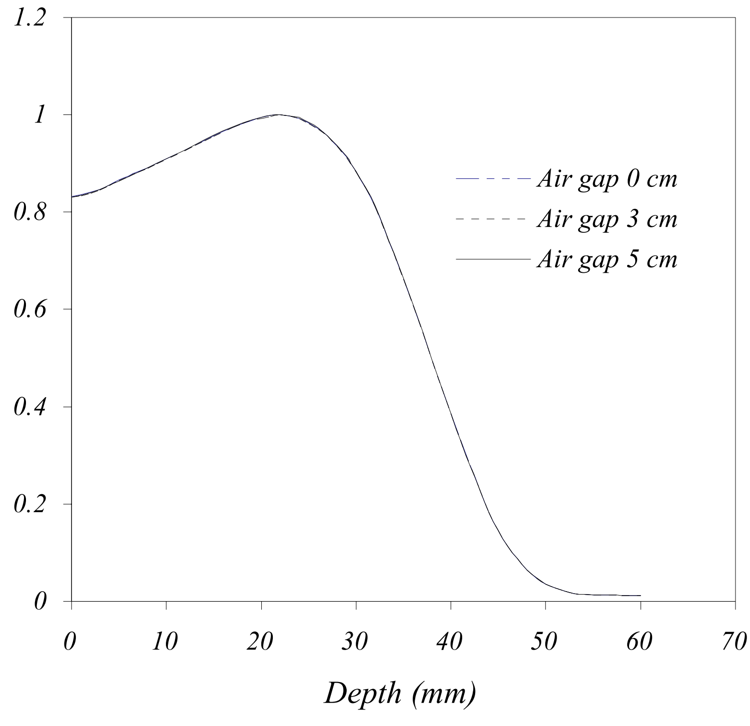

1.2
1
0.8
0.6
0.4
0.2
0
0
10
20
30
40
50
60
70
Depth (mm)
Air gap 0 cm
Air gap 3 cm
Air gap 5 cm

Fig. 6 b)

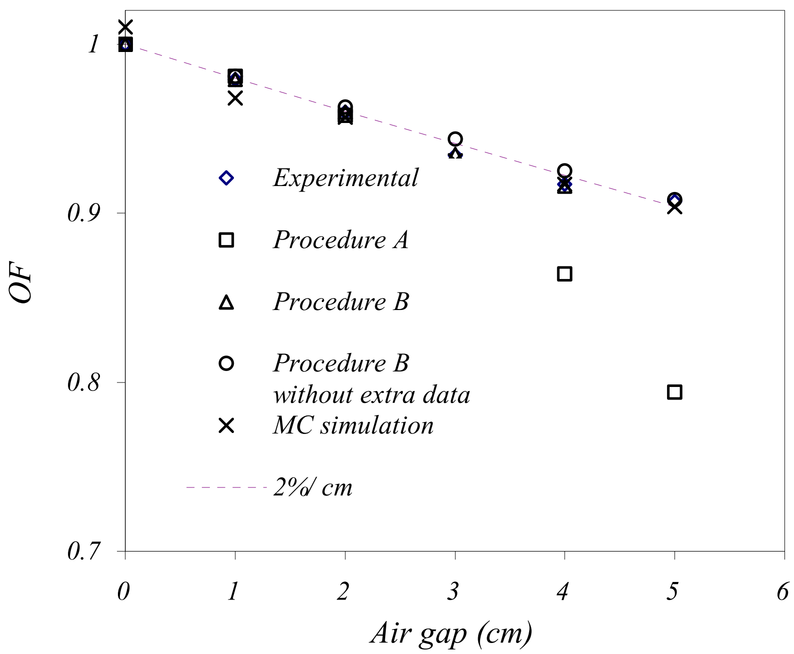
1
0.9
0.8
0.7
OF
0
1
2
3
4
5
6
Air gap (cm)
Experimental
Procedure A
Procedure B
Procedure B
without extra data
MC simulation
2%/ cm

Fig. 7 a)

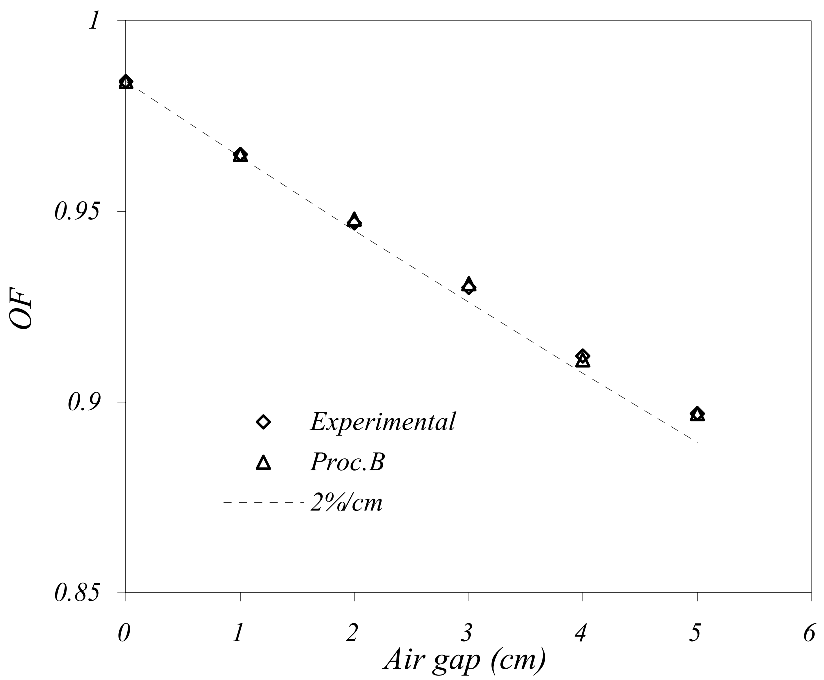
1
0.95
0.9
0.85
OF
0
1
2
3
4
5
6
Air gap (cm)
Experimental
Proc.B
2%/cm

Fig. 7 b)

Table 1

E (MeV)	$\sigma_{\theta x}$ exp. (rad)	$\sigma_{\theta x}$ Proc.A (rad) (FMCS=1)	$\sigma_{\theta x}$ Proc.B (rad) (FMCS=2)	$\sigma_{\theta x}$ MC (rad)
6	0.066	1.1	0.16	0.060
8	0.054	0.6	0.12	0.052
10	0.046	0.4	0.1	0.044
12	0.039	0.32	0.08	0.041
15	0.032	0.2	0.07	0.037
18	0.027	0.15	0.06	0.035

Table 2

Air gap	Exp.	Proc.A	ProcA+input data	Proc.B
0	1	1	1	1
1	0.977	0.976	0.978	0.975
2	0.958	0.925	0.965	0.955
3	0.940	0.836	0.964	0.938
4	0.923	0.729	0.966	0.921
5	0.906	0.623	0.968	0.905